SCHLIEREN SIMULATION OF INTERNAL (m = 1) MHD MODE PERTURBATIONS

G. Lisitano

IPP III/92 September 1983

MAX-PLANCK-INSTITUT FÜR PLASMAPHYSIK

8046 GARCHING BEI MÜNCHEN

MAX-PLANCK-INSTITUT FÜR PLASMAPHYSIK

GARCHING BEI MÜNCHEN

SCHLIEREN SIMULATION OF INTERNAL (m = 1) MHD MODE PERTURBATIONS

G. Lisitano

IPP III/92 September 1983

Die nachstehende Arbeit wurde im Rahmen des Vertrages zwischen dem Max-Planck-Institut für Plasmaphysik und der Europäischen Atomgemeinschaft über die Zusammenarbeit auf dem Gebiete der Plasmaphysik durchgeführt.

IPP III/92 G. Lisitano SCHLIEREN SIMULATION OF INTERNAL (m = 1) MHD MODE PERTURBATIONS

September 1983
(in English)

Abstract

Numerical calculation of schlieren-deflected millimetre-wave probing beams simulates the x-ray emissivity of the hot centre and the local shear of the ploloidal magnetic field during m = 1 perturbations. This allows reproduction of the complicated structures of x-ray signals observed experimentally.

Schlieren Simulation of Internal (m = 1) MHD Mode Perturbations

G. Lisitano
EURATOM - IPP Association
Max-Planck-Institut für Plasmaphysik
8046 Garching bei München (Federal Republic of Germany)

Numerical calculation of schlieren-deflected millimetre-wave probing beams simulates the x-ray emissivity of the hot centre and the local shear of the poloidal magnetic field during m = 1 perturbations. This allows reproduction of the complicated structures of x-ray signals observed experimentally.

PACS numbers: 52.35. Py, 52.65.+z, 52.70.Gw

Growing oscillations of soft-x-ray emission have been identified as due to current-driven m = 1 tearing modes, which are believed to be the cause of internal current disruptions in tokamaks /1,2,3/. With the growth rate of the emissivity oscillations as a basis, the growth of an m = 1 magnetic island and the radial motion of the hot central peak till its annihilation have been invoked in models to explain these disruptions /3,4,5/.

To simulate the radial dependence and growth rate of the m = 1 oscillations, the shear of the poloidal magnetic field $\alpha \equiv \alpha\ (dq/dt)$ and plasma resistivity effects were introduced in the usual model /3/, where the amplitude $\tilde{A}$ of the oscillations relative to the unperturbed emissivity A is expressed by

$$\tilde{A}/A = \int_s Y(\alpha)ds = \int_s Y_T(dT/dx)ds, \qquad (1)$$

s being the line of sight of an x-ray diode.
If a parabolic radial profile is assumed for T_e, the shear parameter dT_e/dx, transversal to s, reproduces the observed radial dependence of the oscillation amplitude. The latter has a minimum at the centre for $dT_e/dx = 0$ and a maximum a few cm from the centre where dT_e/dx is maximum. The time depencence of the growth rate $Y_T(\alpha,t)$ is dependent on the implication of the model /3/ that β_θ and α are also functions of time. For the asymmetric shear parameters, however, the shear

effetcs may be obscured by the integral taken along the line of sight /8/. This makes reproduction of observed perturbations very cumbersome and has not yet allowed clear interpretation of the wide variety of fluctuations ranging from purely ω, 2ω and 3ω bahaviour to several complicated double-peaked structures with evenly and unevenly spaced peaks /6,7/.

In the following, schlieren calculations in the form /9/

$$\Delta A/A = K\int_s F(dN_e/dx)ds,$$

which is numerically similar to the poloidal field shear, reproduce the complicated structure of the experimentally observed m = 1 soft-x-ray wave forms simply by radial displacement and rotation of the hot centre, without the time dependence and fitting problems of the various parameters encountered in other simulation models. In the above expression ΔA is the intensity of the schlieren-deflected electromagnetic rays, A is the total amplitude of the undeflected rays, and N_e is the local plasma density. The schlieren method is only applied to simulate the observed m = 1 fluctuations of the x-rays. The possibility of simulating the sawteeth of internal current disruptions is not considered.

As is well known, the schlieren calculation of a ray path deflected in a dispersive medium is derived from the Fermat law by taking the minimum of the integral $\int_s k\, dl$, where k is the wave number. When this k is replaced by that given by the dispersion relation of an ordinary wave, the radius of curvature R of the deflected ray path is expressed by /10/

$$\frac{1}{R} = -\frac{\vec{N}}{2}\,\frac{V}{1-V}\,, \qquad (3)$$

where $V = N/N_c$, N being the local density and N_c the cut-off density for the wavelength used, and $\vec{N}$ is the unit vector of the normal to the trajectory. From eq. (3) it is seen that the ray deflection is in the direction of decreasing density, is directly proportional to the density gradient and increases as the density.

If a pencil radiation pattern $I(\theta)$ is assumed for an exploring electromagnetic wave beam, the unperturbed signal at the receiver is $A = 2\int_0^{\mu} I(\theta)d\theta$, where μ is the angular width of the two undeflected external rays of a wave beam impinging on the edges of the receiver antenna.

With a perturbed radiation pattern, the received signal

$\Delta A = \int_{\theta-}^{\theta+} I(\theta)d\theta$ depends on the ray density of the beam inside the two deflected external rays which reach the receiver edges. Analytically, these two rays, which are calculated from eq. 3), are identified by the two angles $\theta+$ and $\theta-$ of the radiation pattern $I(\theta)$, which is approximated by the function

$$I(\theta) = \frac{1}{2}\,(e^{-a\theta^2} + e^{-b\theta^2}). \qquad (4)$$

The amplitude of the normalized schlieren signal is then given by

$$\Omega = \frac{\Delta A}{A} = \frac{\int_{\theta-}^{\theta+} I(\theta)d\theta}{2\int_{o}^{\mu} I(\theta)d\theta}\,, \qquad (5)$$

where the error introduced by the numerically simulated radiation pattern proved to be below the uncertainty limit for the measured data points of an experimental pencil radiation pattern realized for the Pulsator tokamak.

From eq. 5) one immediately sees the advantage of the schlieren method in comparison with other diagnostics or other models for simulating MHD mode perturbations: the detected signal at the receiver antenna does not need to be integrated along the ray path like the x-ray emissivity or the phase shift of an ordinary wave. Any change in the distribution of the density $V(\xi,\eta)$ deflects the ray path as calculated by eqs. 3) to 5) and the signal is the one not deflected from the edges of the receiver antenna. Even small variations of the density distribution at any point of the plasma are detected by a sufficient array of exploring wave beams, which, for fusion plasma densities of $N_e \approx 10^{14}$ cm^{-3}, are most sensitive in the millimetre wavelength range /9/.

In view of the asymmetric situations that must be faced by the model all the calculations involved in eqs. 3), 4) and 5) were referred to orthogonal coordinates ξ,η. The density distribution $V(\xi,\eta)$ is then expressed by

$$V(\xi,\eta) = Vo\,\{1 - [\frac{(\xi-\tau\cos\Psi_2-\rho\cos\Psi_1)^2+(\eta-\tau\sin\Psi_2-\rho\sin\Psi_1)^2}{1+\tau^2-2\tau\cos\Psi_2(\xi-\rho\cos\Psi_1)-2\tau\sin\Psi_2(\eta-\rho\sin\Psi_1)}]^{f}\} \qquad (6)$$

where $V_o = N_o/N_e$ is the normalized maximum density values, τ is the radial coordinate of V_o, $\tau\cos\Psi_2$ is the vertex abscissa, Ψ_2 is the angle of V_o, Ψ_1 is the angle of the plasma centre and ρ its radial

coordinate, and f is a profile-flattening index.

Figure 1 shows the isodensity lines and the labelling of the density distribution parameters of eq. 6). The geometrical arrangement of the exploring millimetre-wave pencil beams of the Pulsator tokamak is also sketched in Fig. 1. For a symmetric and centred density distribution, viz. $\tau = 0$ and $\rho = 0$ in Fig. 1, the results of the numerical model were compared with the Shmoys model /11/ valid for a centred and parabolic radial density distribution only. The results of the two models deviated less than 1 %. A detailed description of the numerical program /12/ of the model will be reported elsewhere, the aim of this work being to show that the schlieren method can give an insight into localized MHD phenomena inside the plasma, as shown in the following application of the model.

Figure 2 presents the Ω values calculated from eqs. 4) and 5) for a parabolic and centred density distribution for the three values $V_o = 0.2$, 0.5 and 0.8. It is seen from Fig. 2 that by choosing a convenient density distribution it is possible to obtain an unperturbed schlieren signal intensity, Ω versus radius, which is numerically equal to that, I_o vs radius, of the unperturbed x-ray source, as reported in, for examples, Fig. 6 of Ref. 13.

Although the schlieren method allows simulation of the x-ray emissivity of the hot centre from a given radial density distribution, the following density distributions were chosen in order to simulate some possible physical processes underlying the observed fluctuations of soft-x-ray signals. In this context particular interest is shown in a central density peak radially displaced from the geometrical centre of the discharge tube as shown in the example in Fig. 1. The rotation of such a peak density simulates soft-x-ray signals relating to observed MHD perturbations. The various examples of individual situations shown in Fig. 3 are meant to be combined to provide a possible physical understanding of the observed signals.

In Fig. 3 the centre core of a centred, symmetric and parabolic density profile was radially displaced at $\tau = 0.25$, 0.5 and 0.75 for the three values $V_o = 0.2$, 0.5 and 0.8. The displaced central core is then rotated around the centre of the discharge tube and the calculated schlieren signals for the vertical chords at r/a = 0, $\pm$ 0.25, $\pm$ 0.5, $\pm$ 0.75 are obtained. The rotation was kept centred

at the geometric centre in order to have individual situations closer to the symmetric measurements above and below the equatorial plane reported in Refs. /6,8/.

Features of a dominant m = 1 are evident in the theoretically derived wave forms in Fig. 3. Especially for V_o = 0.5 and 0.8 these wave forms are very similar to those experimentally observed in PLT and ISX-B and reported in Refs. 6 and 8. The only difference between the theoretically derived wave forms in Fig. 3 and those in Refs. 6 and 8 is that in our model the growing amplitude of the m = 1 activity is a function of the radial displacement τ of the centre core, whereas in the experimentally observed m = 1 activity reported in Refs. 6 and 8 the growing amplitude is a function of time. In Fig. 3 the wave forms at r/a = + 0.5 and + 0.75, being the mirror images of those at r/a = - 0.5 and - 0.75, are not shown. For the calculations of Fig. 3 the radiation pattern of the λ = 2 mm wave antennae and the plasma radius a = 11 cm of the Pulsator tokamak were assumed.

Additional fine-grained details of the radial displacement model in Fig. 3 are common to the x-ray measurements reported in Refs. 6 and 8: 1) The channel nearest the centre shows the expected dominant 2ω resulting from m = 1. Successive peaks on centre are not of equal amplitude, a feature that results in the model calculation from the intrinsic simulation of the shear term dT/dx 2) The double humps on positive half-cycles at nearby channels, e.g. r/a = $\pm$ 0.25, are not equal either and the ordering of the inequality reverses between the two channels. These features are again the result of the shear term due to the centre core displacement. If counter-rotation is assumed in the model, the theoretical traces of symmetric channels r/a = $\pm$ 0.25 and $\pm$ 0.5 are exchanged 3) At channels r/a = $\pm$ 0.75, the wave forms are triangular in nature and are again reversed between symmetric channels. The triangular wave forms are outside the q = 1 surface and depend on the large displacement $\tau \geq 0.5$ of the central core.

Note in Fig. 3 that the growing amplitude of the m = 1 wave forms occurs for the channels at large radius, whereas in the central region persistence of the signal amplitude is observed. This persistence of the signal in the central region is also experimentally observed in the emissivity oscillations of soft-x-rays reported in Refs. 6 and 8.

In Fig. 3 no attempt was made to fit the numerically derived data

to the experimental data reported in Refs. 6 and 8. The "emissivity" used is that simulated in Fig. 2 for a parabolic density distribution. Of course, a refined fit could be obtained if a more refined simulation of the x-ray source emissivity was obtained by choosing a more convenient density distribution. Nonetheless, the radial displacement $\tau = 0.75$ provided in Fig. 3 for the appearance of triangular wave forms compares well with a central core displacement of about 10 cm reported in Ref. 6 for the PLT tokamak. This is deduced from the maximum amplitude of the triangular wave form of the soft x-rays observed at r = 16 cm in PLT /6/.

To summarize, the key point of the numerical calculations shown in Fig. 3 is that they clearly demonstrate that the model of central-core radial displacement reproduces well the observed behaviour of soft-x-ray signals without the cumbersome fitting of time-dependent parameters such as shear, resistivity and poloidal field strength faced in other simulation models.

The dichotomy of a millimetre-wave pencil beam which reproduces observed fluctuations of x-ray emission from the hot centre is clearly dependent on the intrinsic property of the schlieren method that it simulates local shear of the poloidal magnetic field for any pressure distribution in the plasma interior.

Besides simulating MHD perturbations, the schlieren reproduction of x-ray signals, presented for the first time in this paper, may provide a powerful tool for studying variations of the local pressure distribution in hot plasmas preceding the onset of current disruptions.

REFERENCES

1 S. von Goeler, W. Stodiek, and N.R. Sauthoff, Phys. Rev. Lett. 33, 1201 (1974).

2 R.B. White, D.A. Monticello, and M.N. Rosenbluth, Phys. Rev. Lett. 39, 1618 (1977).

3 G.L. Jahns, M. Soler, B.V. Waddel, J.D. Callen, and H.R. Hicks, Nucl. Fus. 18, 609 (1978).

4 R.B. White, D.A. Monticello, M.N. Rosenbluth, and B.V. Waddel, in Proceedings of the 6th Int. Conf. on Plasma Physics and Controlled Nuclear Fusion Research, Berchtesgaden, Germany, 1976 (International Atomic Energy Agency, Vienna, 1977), Vol. I, p. 659.

5 B.V. Waddel, G.L. Jahns, J.D. Callen, and H.R. Hicks, Nucl. Fus. 18, 735 (1978).

6 N.R. Sauthoff, S. von Goeler, D.R. Eames, and W. Stodiek, in Proceedings of the International Atomic Energy Agency Symposium on Current Disruption in Toroidal Devices, Max-Planck-Institut für Plasmaphysik Report No. IPP 3/51, 1979 (unpublished), paper C-5.

7 B.V. Waddel, M.N. Rosenbluth, D.A. Monticello, and R.B. White, Nucl. Fus. 16, 528 (1976).

8 J.L. Dunlap, B.A. Carreras, V.K. Paré, J.A. Holmes, S.C. Bates, J.D. Bell, H.R. Hicks, V.E. Lynch, and A.P. Navarro, Phys. Rev. Lett. 48, 538 (1982).

9 G. Lisitano, in Diagnostics for Fusion Experiments (E. Sindoni and G. Wharton, eds.) Pergamon Press, Oxford, New York (1979) p. 223.

10 L.D. Landau, E.M. Lifchitz, Pergamon Press, Oxford (1975).

11 J. Shmoys, J.Appl. Phys. 32, 689 (1961).

12 G. Lisitano, F. Baretich, G.Gammino, I. Bazzo, C. Cassamagnaghi, and S. Santicchi, in Proceedings of the 11th European Conference on Plasma Physics and Controlled Nuclear Fusion, Aachen, 1983, Vol. 7D, Part II, p. 89.

13 S. von Goeler, in Proceedings of the 7th European onference on Plasma Physiks and Controlled Nuclear Fusion, Lausanne, 1975, Vol. I, p.71.

FIGURE CAPTIONS

Fig. 1 Isodensity lines with the parameter labelling of eq. 6).

Fig. 2 Schlieren signals Ω vs radius for a parabolic radial density distribution.

Fig. 3 Schlieren signals for radially displaced density centre core, τ = 0.25, 0.5, 0.75, and peak density values V_o = 0.2, 0.5, 0.8 for λ = 2 mm wave pencil beams positioned at r/a = 0, $\pm$ 0.25, $\pm$ 0.5 and $\pm$ 0.75.

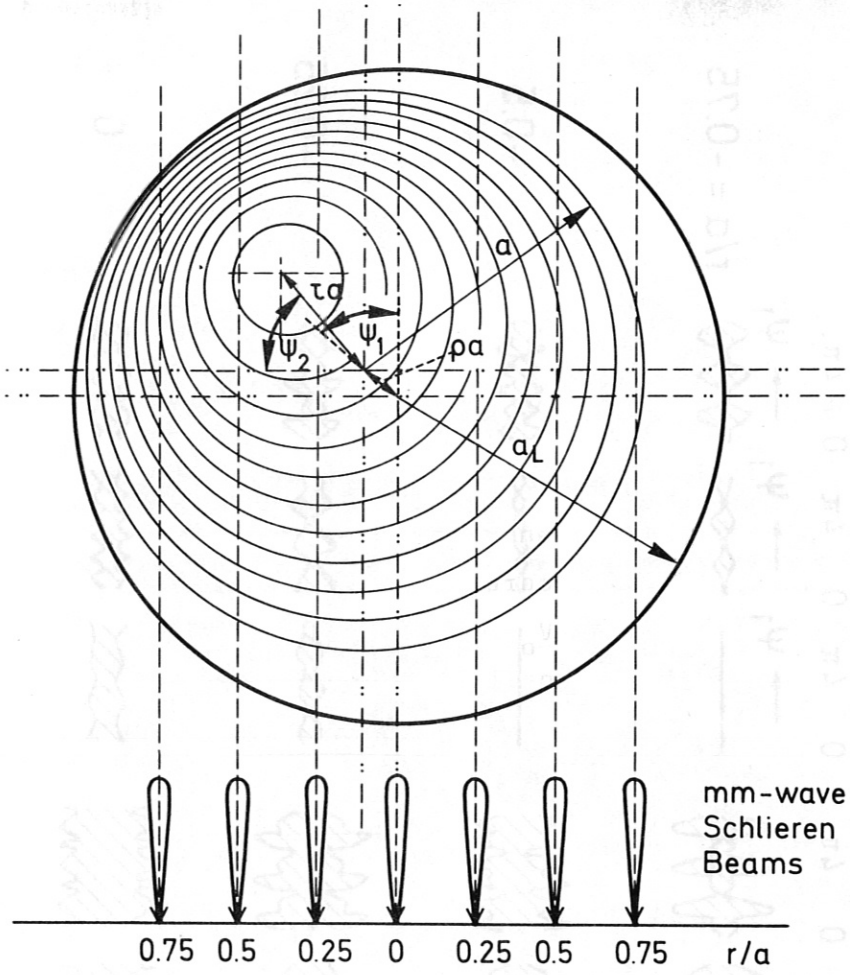
a
τa
ψ1
ψ2
ρa
aL
mm-wave
Schlieren
Beams
0.75 0.5 0.25 0 0.25 0.5 0.75 r/a

Fig. 1

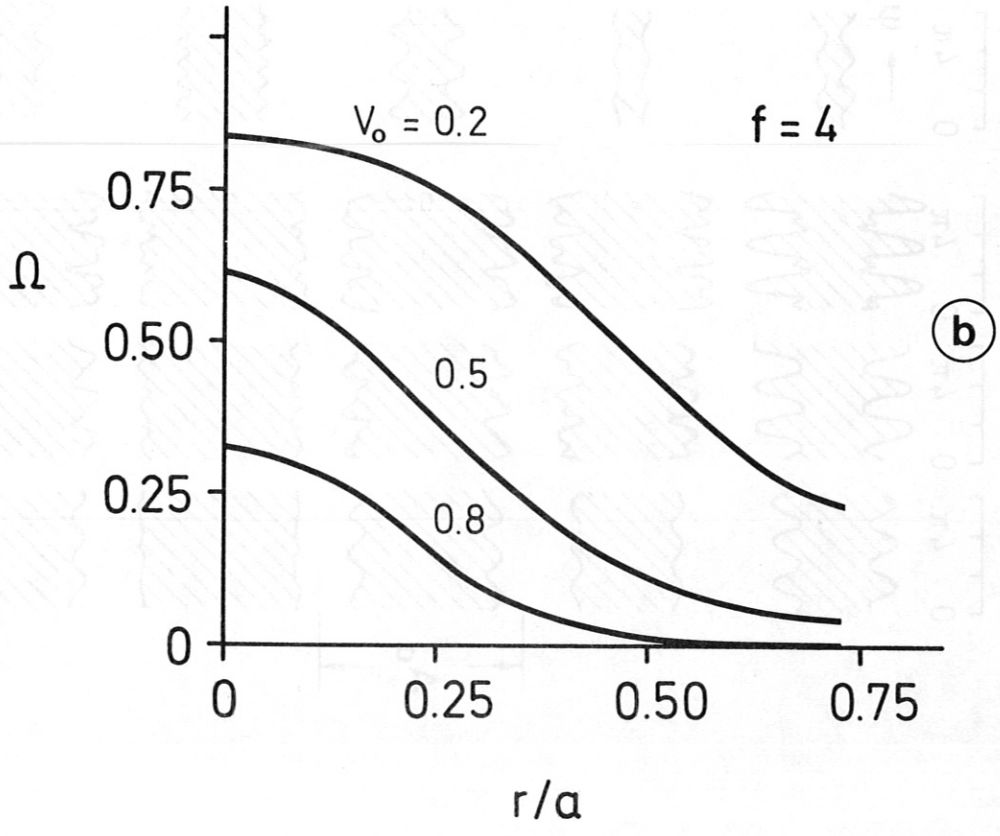
Vo = 0.2
f = 4
Ω
0.75
0.50
0.25
0
0.5
0.8
b
0 0.25 0.50 0.75
r/a

Fig. 2

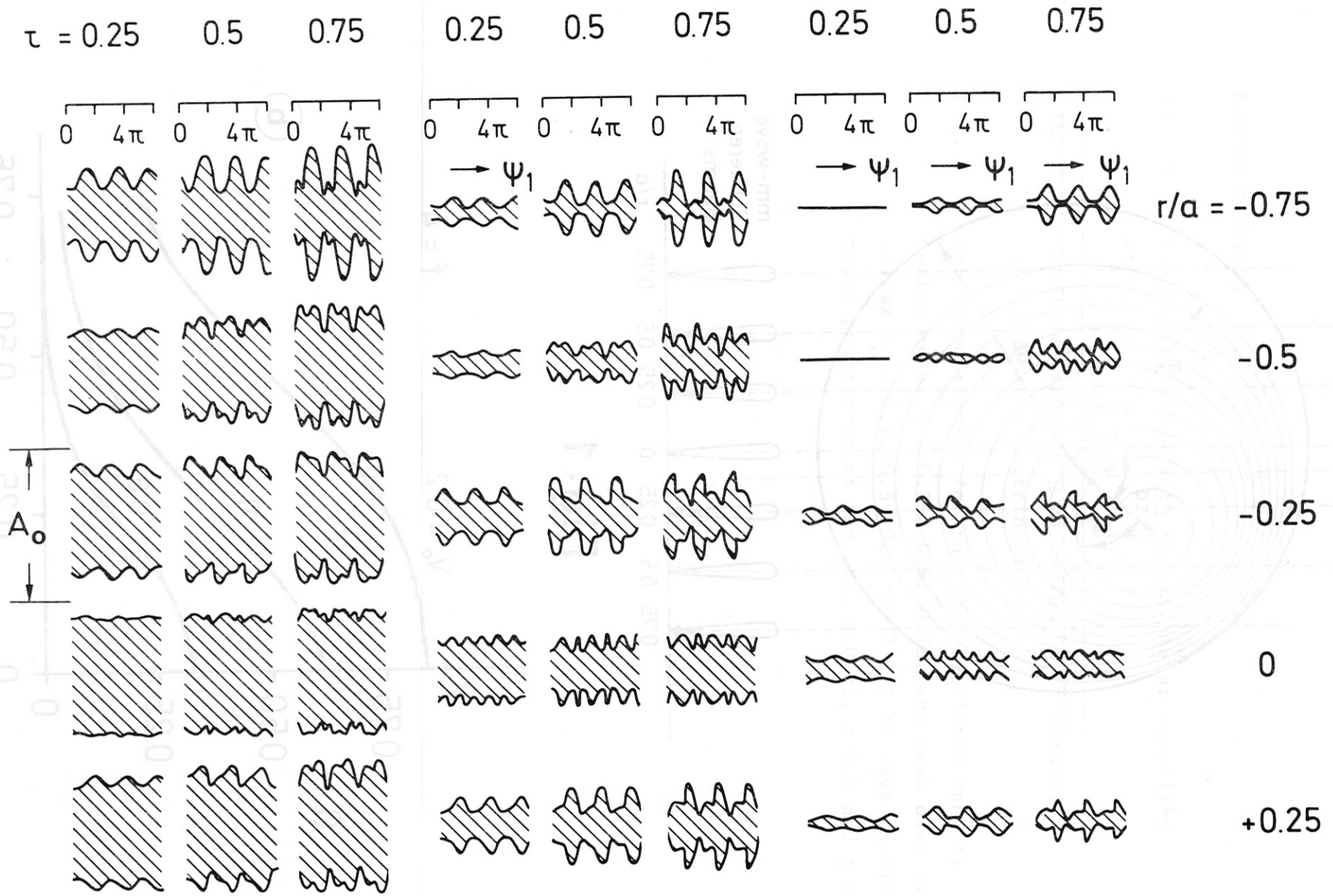

Fig.3

IPP3- LTO 564-83